839. Vibration analysis of geared rotor system under time varying mesh stiffness effects

Ying-Chung Chen[1], Chung-Hao Kang[2], Siu-Tong Choi[3]
[1, 3]Department of Aeronautics and Astronautics Engineering, National Cheng Kung University
Tainan 701, Taiwan, R. O. C.
[2]Graduate Institute of Mechatronic System Engineering, National University of Tainan
Tainan 700, Taiwan, R. O. C.
E-mail: [1]*ycchen80@gmail.com*, [2]*chkang1977@gmail.com*, [3]*choi@mail.ncku.edu.tw*

(Received 13 April 2012; accepted 4 September 2012)

Abstract. The present work contributes to the analysis of the interactions between gears, shafts and journal bearings in a geared rotor-bearing system. Although there are analyses for both of the gear and rotor-bearing system dynamics, the coupling effect of the nonlinear variable pressure angle and geared rotor-bearing system is deficient. In contrast to the majority of the models in the literature, the variable mesh stiffness and pressure angle are introduced in this paper while they were considered as constant in previous models. The equations of motion for the geared rotor-bearing system are obtained by applying Lagrange's equation, and the Runge-Kutta numerical method is used to solve the equations of motion. Numerical results of this study indicated that the proposed model provides realistic dynamic response of a geared rotor-bearing system.

Keywords: gear, rotor system, time varying mesh stiffness.

1. Introduction

The geared rotor-bearing system is one of the main mechanisms for modern power transmission. It is often coupled with bearing systems, power generation and power extraction. On account of the increasing demand for high speed and accurate transportation, the research in the field of geared rotor dynamics is very important. The dynamic analysis of the geared rotor-bearing system with variable pressure angel is investigated in this paper.

The dynamic characteristics of geared rotor-bearing systems have been studied by many researchers [1-4]. Nelson [5] established the shape functions by using Timoshenko beam theory and finite element method, and Bucciarelli [6] presented unbalance response due to instability of rotating shaft. Shiau and Hwang [7] presented a polynomial expansion method for the dynamic analysis of rotor-bearing systems. For geared rotor system, Lund [8] considered the coupling effects of the torsional and lateral vibrations. Iida et al. [9] considered a simple geared system including the coupled torsional and flexural vibration. Neriya et al. [10] extended the model of Iida et al. [9] by representing a single gear with a two mass-spring-damper system. Kahraman et al. [11] developed a finite element model of a geared rotor system. Shiau et al. [12] analyzed the lateral response due to torsional excitation of geared rotor, and Lee et al. [13] developed the coupling of lateral and torsional vibration for the geared rotor-bearing system. The effects of the residual shaft bow and viscoelastic supports were investigated by Kang et al. [14] Kim et al. [15] developed a new dynamic model for the gear set that the pressure angle and the contact ratio as time-varying variables.

2. Modeling of the System

The configuration of a geared rotor-bearing system is shown in Fig. 1. Two uniform flexible shafts are of length L_1 and L_2, and the gear pair is mounted on the shafts. An external torque M exerts upon the driving gear. The contacting mesh force is represented by the gear mesh stiffness k_m and damping c_m along the pressure line. Four bearings are modeled as flexible elements with damping and stiffness denoted as c_j^b and k_j^b. A single shaft system with a rigid disk is shown in

Fig. 2, in which the fixed reference frame, $X-Y-Z$, is used to describe the system motion. Five degrees of freedom V, W, α, B, Γ are considered at each nodal point of the shaft, where V and W are lateral displacements along Y and Z directions, respectively, B and Γ are rotational displacements, α is the torsional displacement, and the axial translational vibration is neglected.

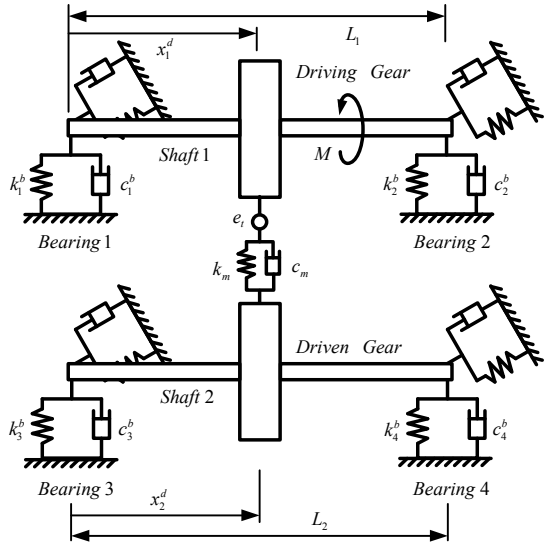

Fig. 1. The configuration of a geared rotor-bearing system

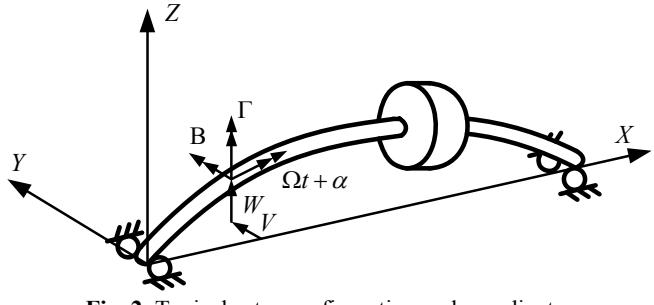

Fig. 2. Typical rotor configuration and coordinates

Fig. 3 shows the configuration and generalized coordinates for the pair of gears [15], which are mounted on the shafts as shown in Fig. 1. The teeth are regarded as flexible cantilever beams and are deformed by both the bending and shear. The mass, transverse mass moment of inertia, polar mass moment of inertia of the driving gear and driven gear are, respectively, m_{d1}, I_{dD1}, I_{dp1} and m_{d2}, I_{dD2}, I_{dp2}. The motion of the gear set can be defined with ten generalized coordinates, which are the same as the node coordinates of two shafts, where the gears are mounted. The dashed and solid circles represent the gear pair before and after motion, respectively. O_1 and O_2 are the initial centers of each shaft, and C_1 and C_2 are the axis centers after the motion. The mass centers of gears are denoted by G_1 and G_2. The magnitudes of the eccentricity denoted by e_1 and e_2, and the eccentricity angles are denoted as Φ_{d1} and Φ_{d2}. The angular coordinates of the driving and driven gears are defined as:

$$\theta_i(t) = \pm\Omega_i t + \alpha_{di}(t) + \Phi_{di} \tag{1}$$

where $i = 1$ and 2 mean the driving and driven gears, respectively. Ω_i are the spin speeds of shaft. The displacement vectors for the mass centers of the gears are defined as:

$$\hat{r}_i(t) = [V_{di}(t) + e_i \cos\theta_i(t)]\hat{j}_i + [W_{di}(t) + e_i \sin\theta_i(t)]\hat{k}_i \tag{2}$$

where $\hat{j}_i$ and $\hat{k}_i$ are the unit vectors in X_i and Y_i axes. The distance between centers, d, is changed to d' after the motion, and d' is defined as:

$$d'(t) = \sqrt{[V_{d2}(t) - V_{d1}(t) + d]^2 + [W_{d2}(t) - W_{d1}(t)]^2} \tag{3}$$

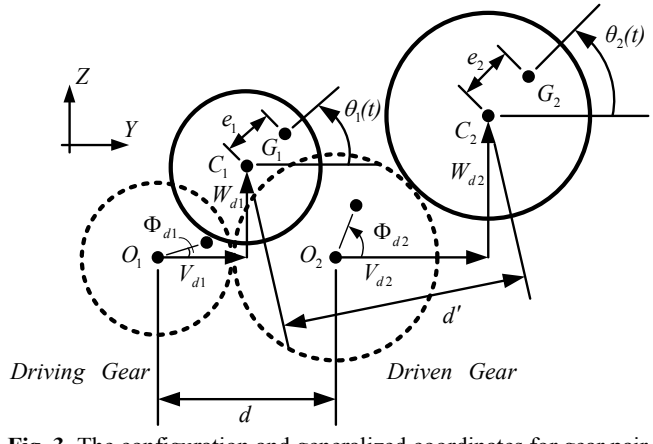

Fig. 3. The configuration and generalized coordinates for gear pair

In Fig. 4, the gear pair is modeled as the equivalent stiffness k_m and damping c_m with transmission error $e_t(t)$ along the pressure line between the teeth. The equivalent stiffness and damping are treated as time-varying coefficients in this paper. The pressure line is defined as the common tangent line of the base circles for the gear set, and the pressure angle ϕ_p is defined as:

$$\phi_p(t) = \cos^{-1}[(R_1 + R_2)/d'(t)] \tag{4}$$

where R_1 and R_2 are the radii of base circles of gears.

The angle of the driven gear relative to the driving gear is represented by:

$$\psi(t) = \tan^{-1}[(W_{d2} - W_{d1})/(V_{d2} - V_{d1} + d)] \tag{5}$$

The pressure angle and the gear position angle in this paper are affected by the translational motions of the gear pair while the previous studies neglected these effects. According to the above assumption that the gear mesh is modeled as the equivalent stiffness and damping with transmission error, the gear mesh deformation along the pressure line can be written as:

$$\delta(t) = (V_{d2} - V_{d1})\sin(\phi_p - \psi) + (W_{d2} - W_{d1})\cos(\phi_p - \psi) - (R_1\alpha_{d1} + R_2\alpha_{d2}) + e_t \tag{6}$$

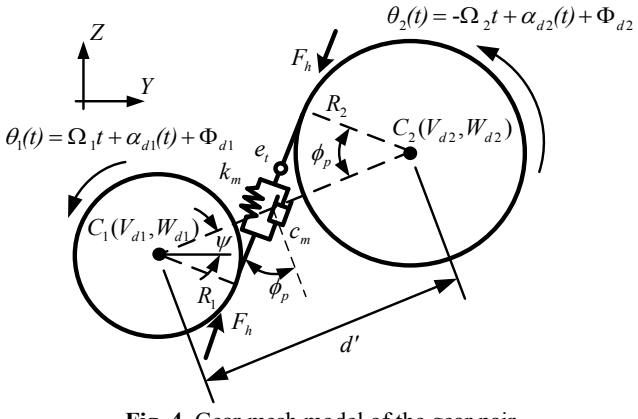

Fig. 4. Gear mesh model of the gear pair

Thus, the gear mesh force along the pressure line can be expressed as:

$$F_h(t) = k_m\delta + c_m\dot{\delta} \tag{7}$$

The mesh stiffness model in Kahraman et al. [11] is used in this paper, and is described as a periodic function with mesh period T_m in Fig. 5. The succeeding pair of teeth should contact immediately when one pair of teeth lose the contact with each other. The contact ratio m_p is presented to measure this overlapping action. There are two pairs of contacting teeth when time *t* is in the range from $(n-1)T_m$ to $(m_p + n - 2)T_m$, and k_u is the maximum mesh stiffness in this mesh process. There is only one pair of contacting teeth if *t* is in the range from $(m_p + n - 2)T_m$ to nT_m, and k_l is the minimum mesh stiffness. The definitions of T_m and m_p are defined as:

$$T_m = 2\pi / N_1\Omega_1 = 2\pi / N_2\Omega_2 \tag{8}$$

$$m_p(t) = [\sqrt{A_1^2 - R_1^2} + \sqrt{A_2^2 - R_2^2} - d\sin\phi_p(t)] / p_b \tag{9}$$

where N_1 and N_2 are the numbers of teeth for gears, A_1 and A_2 are the radii of the addendum circles, and p_b is the base pitch.

3. Governing Equation of the System

The components of this geared rotor-bearing system include the gear pairs, bearing supports and rotor shafts. The equations of motion are derived for each component as follows.

The gear pair in this paper is assumed as two disks, so the kinetic energies of driving gear and driven gear can be described as:

$$T_i^g = [m_{di}\dot{\hat{r}}_i^2 + I_{dp,i}(\pm\Omega_i + \dot{\alpha}_{di})^2 + I_{dD,i}\dot{\mathrm{B}}_{di}^2 + I_{dD,i}\dot{\Gamma}_{di}^2 + I_{dp,i}(\pm\Omega_i + \dot{\alpha}_{di})(\dot{\mathrm{B}}_{di}\Gamma_{di} - \dot{\Gamma}_{di}\mathrm{B}_{di})]/2\,. \tag{10}$$

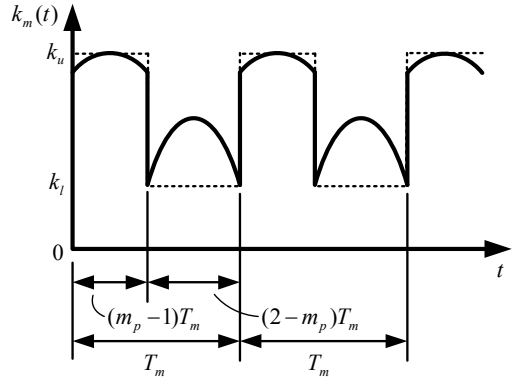

Fig. 5. Non-linear stiffness model with mesh period

The components of the gear mesh forces on the driving gear and the moment about the geometric center can be expressed:

$$F_{hy1} = -F_h \sin(\phi_p - \psi) = -(k_m \delta + c_m \dot{\delta}) \sin(\phi_p - \psi) \tag{11}$$

$$F_{hz1} = -F_h \cos(\phi_p - \psi) = -(k_m \delta + c_m \dot{\delta}) \cos(\phi_p - \psi) \tag{12}$$

$$T_{h1} = -R_1 F_h = -R_1 (k_m \delta + c_m \dot{\delta}) + M \tag{13}$$

For the driven gears, similar expressions can be obtained by applying the Lagrange approach and neglecting the transmission error, the equations of motion of the gear pair can be obtained:

$$[M_d]\{\ddot{q}_d\} + ([G_d] + c_m[C_d])\{\dot{q}_d\} + (k_m[K_{d1}] + c_m \dot{\Phi}[K_{d2}])\{q_d\} = \{F_d\} \tag{14}$$

where $\{q_d\} = \{V_{d1} \quad W_{d1} \quad \mathrm{B}_{d1} \quad \Gamma_{d1} \quad \alpha_{d1} \quad V_{d2} \quad W_{d2} \quad \mathrm{B}_{d2} \quad \Gamma_{d2} \quad \alpha_{d2}\}^T$.

For shafts, two-noded element is used for the finite element formulation in this paper. As is shown in Fig. 6, five degrees of freedom are considered at each nodal point. The kinetic energy and potential energy of the shaft element can be expressed as:

$$T^e = 1/2 \times \int_0^l \{\rho A(\dot{V}_s^2 + \dot{W}_s^2) + I_{sD}(\dot{\mathrm{B}}_s^2 + \dot{\Gamma}_s^2) + I_{sP}(\Omega_1 + \dot{\alpha}_s)^2 + I_{sP}(\Omega_1 + \dot{\alpha}_s)(\dot{\mathrm{B}}_s \Gamma_s - \dot{\Gamma}_s \mathrm{B}_s)\} ds \tag{15}$$

$$U^e = 1/2 \times \int_0^l \{EI[(\mathrm{B}_s')^2 + (\Gamma_s')^2] + GI_{sP}(\alpha_s')^2 ds + \kappa' GA[(V_s' - \Gamma_s)^2 + (W_s' + \mathrm{B}_s)^2]\} ds \tag{16}$$

where ρ, A, I, I_{sD}, I_{sP}, E, G and κ' are the parameters and modulus of the shafts[12]. By Lagrange approach, the motion equations of shaft elements can be obtained:

$$[M^e]\{\ddot{q}^e\} + \Omega[G^e]\{\dot{q}^e\} + [K^e]\{q^e\} = 0 \tag{17}$$

where $\{q^e\} = \{V_{e1} \quad W_{e1} \quad \mathrm{B}_{e1} \quad \Gamma_{e1} \quad \alpha_{e1} \quad V_{e2} \quad W_{e2} \quad \mathrm{B}_{e2} \quad \Gamma_{e2} \quad \alpha_{e2}\}^T$.

In this paper, those four bearing supports are assumed as isotropic. The potential energy and virtual work of jth bearing support can be expressed as:

$$U_j^b = (k_j^b V_{bj}^{\ 2} + k_j^b W_{bj}^{\ 2})/2 \text{ and } \delta W_j^{nc} = -c_j^b \dot{V}_{bj} \delta V_{bj} - c_j^b \dot{W}_{bj} \delta W_{bj}. \tag{18}$$

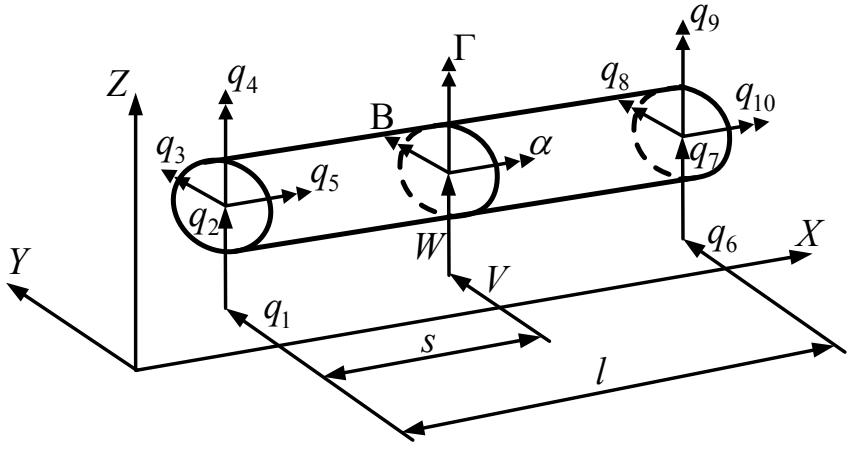

Fig. 6. Shaft element and coordinate system

By the Lagrangian approach, the motion equations of jth bearing support can be obtained as:

$$\begin{bmatrix} c_j^b & 0 \\ 0 & c_j^b \end{bmatrix} \{\dot{q}_j^b\} + \begin{bmatrix} k_j^b & 0 \\ 0 & k_j^b \end{bmatrix} \{q_j^b\} = \begin{Bmatrix} 0 \\ 0 \end{Bmatrix} \tag{19}$$

where $\{q_j^b\} = \{V_{bj} \quad W_{bj}\}^T$ and j =1~4.

The system equation of motion can be obtained by assembling equations of each component in the above, and is expressed as:

$$[M^s]\{\ddot{q}^s\} + [C^s]\{\dot{q}^s\} + [K^s]\{q^s\} = \{F^s\} \tag{20}$$

where $\{q^s\}$ is the state vector, $[M^s]$, $[C^s]$ and $[K^s]$ are the system mass, damping and stiffness matrices, respectively. $\{F^s\}$ is the forcing vector due to the mesh, external torque and eccentricity effects, which includes the non-linear mesh effect.

4. Results and Discussion

In order to compare the results of Kim et al. [15], the eccentricity of the gear is neglected and the torsional bearing dampings c_{t1}, c_{t2} are considered. The parameters of the gear pair and rotor system are shown in refs. [12] and [15]. The rotating speeds of the shafts are considered as constants in this paper, and the acceleration process is neglected. Fig. 7 shows the gear mesh deformations with different rotating speeds when both of the shaft lengths are zero. The equivalent damping $c_{j,equi.}^b$ and stiffness $k_{j,equi.}^b$ in each bearing are $c_{j,equi.}^b = 2c_j^b$, $k_{j,equi.}^b = 2k_j^b$. The amplitudes of those deformations in Fig. 7 are similar to those in Kim et al. [15], and this indicates the accuracy of the simulation in this paper. The details of the deformations are shown in Fig. 8. The differently rotating speeds change the frequency of mesh, and the contact ratio of the mesh is also varied. But the varying of amplitude is unobvious. Because the eccentricity is neglected that the lateral deformations r_1, r_2 are not effected as the varying rotating speed varies.

In the followings, the shaft lengths are considered for $L = 254$ as Shiau's [12], and Ω_1 is

selected as 3000 rpm. Fig. 9 shows the lateral deformation r_1 and gear mesh deformations with/without the rotating shaft. In the above figures, the equivalent damping $c^b_{j,equi.}$ and stiffness $k^b_{j,equi.}$ are selected as $c^b_{1,equi.} = 5.6$, $c^b_{2,equi.} = 8.4$ (Ns/m) and $k^b_{j,equi.} = 106$ (N/m). The solid lines in Fig. 9 and Fig. 10 mean the geared rotor-bearing system with shaft $L = 254$, and the dashed lines mean the shaft $L = 0$ respectively. In this paper the damping and stiffness coefficients, c^b_j and k^b_j, are assumed as the same value, c_b and k_b. As the shown in Fig. 9(a), the system with shaft $L = 254$ is not convergent before 0.02 sec. as the damping is selected as 2.8 and 4.2. (The equivalent damping coefficients $c^b_{1,equi.}$ and $c^b_{2,equi.}$ are 5.6 and 8.4 as in Kim et al. [15].) Fig. 9(a) also shows the lateral deformation with different damping coefficients, which effects the amplitude and convergence time for the vibration of lateral deformation. This geared rotor-bearing system with shaft $L = 254$ can be convergent effectively same as the system $L = 0$ when the damping coefficients are selected as $c_b = 800$ (Ns/m) . It means if the time-varying gear mesh stiffness and pressure angle in 2-D plane as Kim et al. [15] are considered into the 3-D geared rotor-bearing system in this paper, the damper should be redesigned. Fig. 9(b) shows the detail of the gear mesh deformation. The frequency content of responses is more complex when the time-varying mesh effect is considered as the system in this paper. However, as shown in Fig. 9(b), the mesh periods T_m are the same for system with/without the rotating shaft.

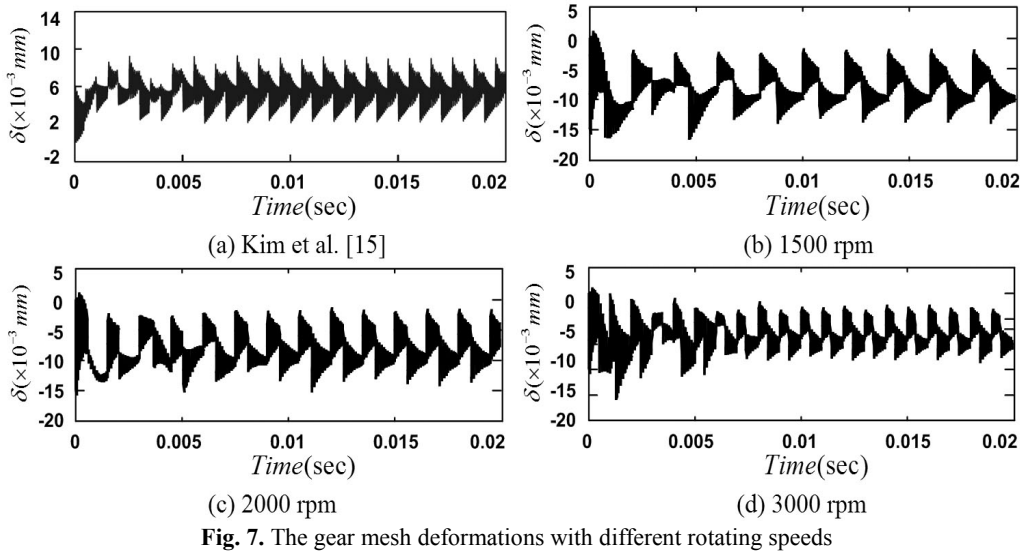

Fig. 7. The gear mesh deformations with different rotating speeds

Fig. 10 shows the lateral deformations r_1 , r_2 with different bearing stiffness. In Fig. 10, damping coefficients c^b_j are selected as 1000 Ns/m. Comparing the dashed lines and solid lines in Fig. 10(a) and Fig. 10(b) with $k^b_{1,equi.} = k^b_{2,equi.} = 10^6$ N/m and $k_b = 5 \times 10^5$ N/m, the magnitudes of lateral deformations in steady state are increased when the rotating shaft $L = 254$ is considered. For the reason that the shafts are flexible, this will increase the deformations of the gears. Especially while the gear pair is mounted at the middle of the shaft. In Fig. 10(a) and Fig. 10(b), increasing the bearing stiffness can reduce the magnitudes of lateral deformations r_1 , r_2 in steady state effectively.

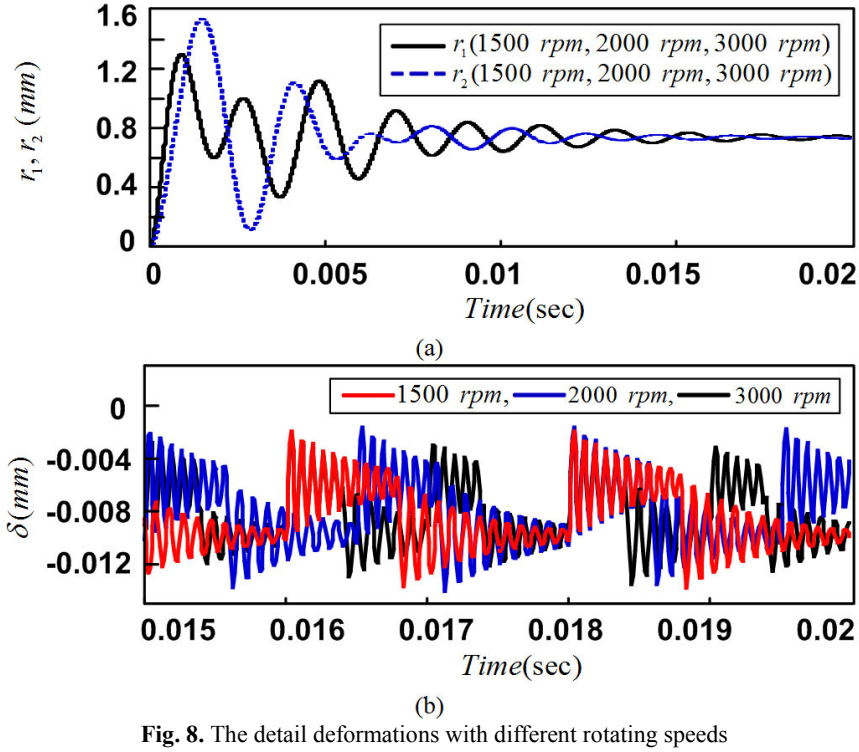

Fig. 8. The detail deformations with different rotating speeds

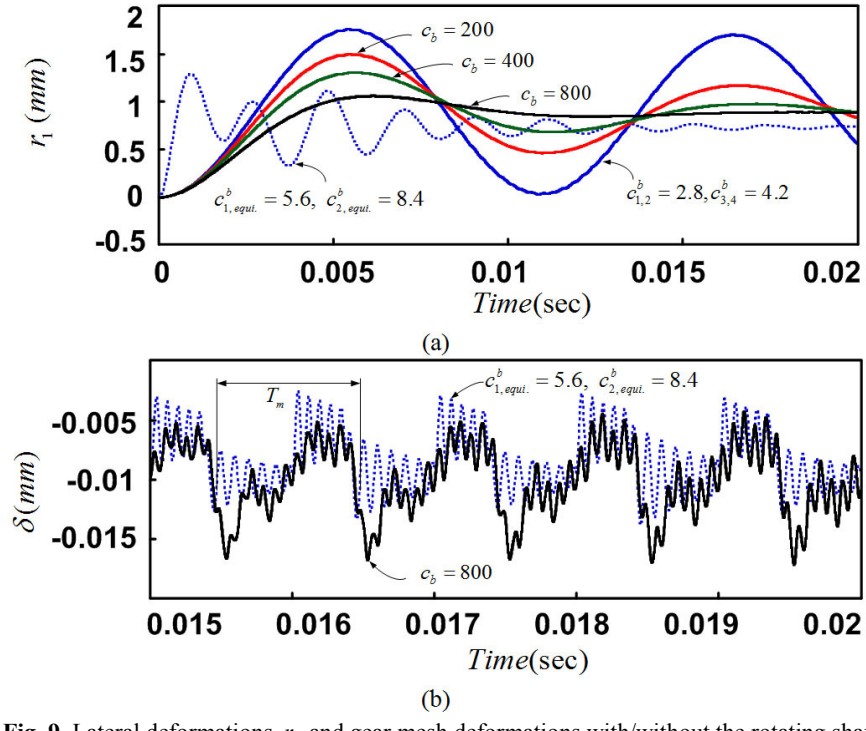

Fig. 9. Lateral deformations r_1 and gear mesh deformations with/without the rotating shaft

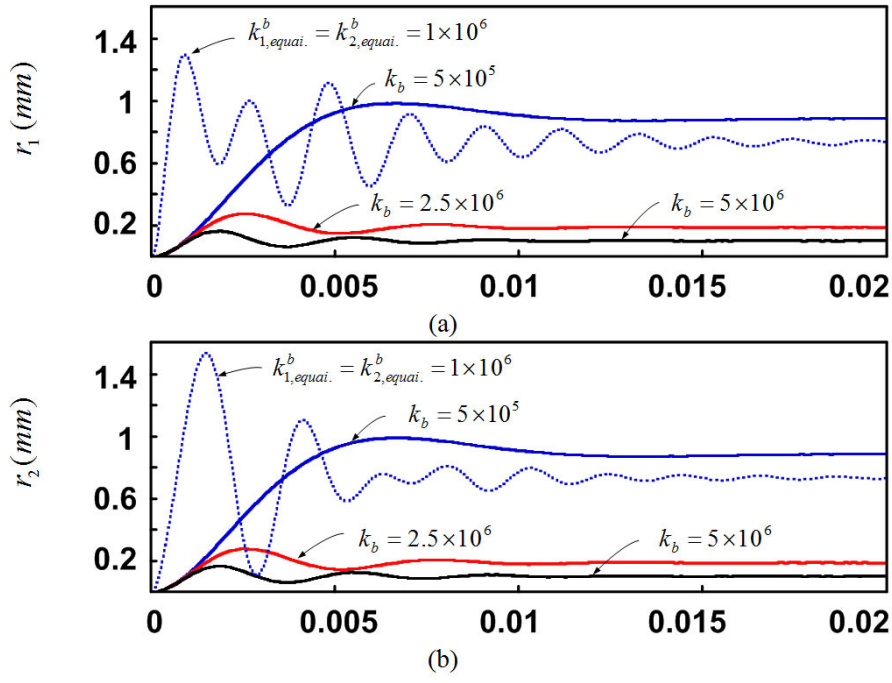

Fig. 10. Lateral deformations r_1, r_2 and gear mesh deformations with different bearing stiffness

5. Conclusions

The geared rotor-bearing system is one of the main mechanisms for modern power transmission. This paper investigates the dynamic responses by considering the couple effect of the time-varying mesh and geared rotor-bearing system, for it is deficient in the previous researches. The time-varying mesh effects include the pressure angle and contact ratio while the previous model has regarded them as constants. As the results show, the damper coefficient should be redesigned when this effect of time-varying gear mesh in 2-D plane are considered into the 3-D geared rotor-bearing system. Moreover, the mesh periods T_m are the same for systems with/without the rotating shaft.

References

[1] **Lund J. W., Sternlicht B.** Rotor-bearing dynamics with emphasis on attenuation. Journal of Basic Engineering, Vol. 84, 1962, p. 491-502.
[2] **Dworski J.** High-speed rotor suspension formed by fully floating hydrodynamic radical and thrust bearings. Journal of Engineering for Power, Vol. 86, 1964, p. 149-158.
[3] **Gunter E. J.** Influence of flexibility mounted rolling element bearings on rotor response, part 1: linear analysis. Journal of Lubrication Technology, ASME, Vol. 92, 1970, p. 59-67.
[4] **Childs D. W., Graviss K.** A note on critical-speed solutions for finite-element-based rotor models. Journal of Mechanical Design, Vol. 104, 1982, p. 412-418.
[5] **Nelson H. D.** A finite rotating shaft element using Timoshenko beam theory. Journal of Mechanical Design, Vol. 102, 1980, p. 793-803.
[6] **Bucciarelli L. L.** On the instability of rotating shafts due to internal damping. Journal of Applied Mechanics, Vol. 49, 1982, p. 425-428.
[7] **Shiau T. N., Hwang J. L.** Generalized polynomial expansion method for the dynamic analysis of rotor-bearing systems. Journal of Engineering for Gas Turbines and Power, Vol. 115, 1993, p. 209-217.

[8] **Lund J. W.** Critical speed, stability and response of a geared train of rotors. Journal of Mechanical Design, Vol. 100, 1978, p. 535-538.

[9] **Iida H., Tamura A., Kikuch K., Agata H.** Coupled torsional-flexural vibration of a shaft in a geared system of rotors. Bulletin of the JSME, Vol. 23, 1980, p. 2111-2117.

[10] **Neriya S. V., Bhat R. B., Sankar T. S.** Effect of coupled torsional-flexural vibration of a geared shaft system on dynamic tooth load. The Shock and Vibration Bulletin, Part 3, Vol. 54, 1984, p. 67-75.

[11] **Kahraman A., Ozguven H. N., Houser D. R., Zakrajsek J. J.** Dynamics analysis of geared rotors by finite elements. Journal of Mechanical Design, Vol. 114, 1992, p. 507-514.

[12] **Shiau T. N., Choi S. T., Chang J. R.** Theoretical analysis of lateral response due to torsional excitation of geared rotors. Mechanism and Machine Theory, Vol. 33, 1998, p. 761-783.

[13] **Lee A. S., Ha J. W., Choi D. H.** Coupled lateral and torsional vibration characteristics of a speed increasing geared rotor-bearing system. Journal of Sound and Vibration, Vol. 263, 2003, p. 725-742.

[14] **Kang C. H., Hsu W. C., Lee E. K., Shiau T. N.** Dynamic analysis of gear-rotor system with viscoelastic supports under residual shaft bow effect. Mechanism and Machine Theory, Vol. 46, 2011, p. 264-275.

[15] **Kim W., Yoo H. H., Hung J. C.** Dynamic analysis for a pair of spur gears with translational motion due to bearing deformation. Journal of Sound and Vibration, Vol. 329, 2010, p. 4409-4421.

